J. Ind. Geophys. Union ( September 2016 )
**v.20, no.5, pp: 472-481**

# Time-lapse seismic response evaluation based on well log data for Ankleshwar reservoir, Cambay basin, India

**U.Vadapalli* and N.Vedanti**

CSIR – National Geophysical Research Institute, Hyderabad-500007, India
*Corresponding Author: umageo.anm4@gmail.com

**ABSTRACT**

Time-lapse seismic reservoir monitoring can image fluid-flow effects in a reservoir if the changes in seismic properties of the reservoir due to production or on-going recovery processes are large enough to detect. Thus, before acquiring a time-lapse seismic data, it is necessary to carry out feasibility study for time-lapse seismic reservoir monitoring to get an estimated seismic response. In the present study, Gassmann fluid substitution analysis and forward modeling based on well logs have been carried out to predict the seismic response of a paysand of Ankleshwar reservoir, which is being studied for $CO_2$ – EOR. In this reservoir for enhanced oil recovery (EOR), $CO_2$ injection into a paysand of the reservoir is found to be appropriate, taking into cognizance its success in different reservoirs all over the world.

The seismic response of paysand $S_5$ in a well is modelled for different saturations and a variable thickness of $CO_2$ in the paysand. It is observed that because of the first appearance of $CO_2$, sudden drop in acoustic impedance of the paysand would lead to detectable time shift at the top. However, as $CO_2$ occupies full thickness of the paysand time shift at the top is reduced. Time shift at the bottom responds to overall velocity drop in full thickness of the paysand and it could not be detectable. We also inferred that in this case time-lapse time shift analysis would be more helpful compared to the amplitude analysis and it should be possible to image $CO_2$ plume in the reservoir. The replacement of oil and water in the paysand with $CO_2$ might lead to 9% drop in P-wave velocity.

**Key words:** Time-lapse seismic response, Gassmann's equation, fluid replacement modeling, well log data, $CO_2$ injection, $CO_2$ – EOR, Ankleshwar reservoir.

## INTRODUCTION

A reservoir under production and Enhanced Oil Recovery (EOR) observes changes in saturation or pressure or both over the time. For many reservoirs, the effect of change in pore pressure will have a limited effect upon the seismic parameters (Landro 2002). Also the effect of pressure on reservoir properties is not yet fully established (Dimri et al., 2012). Changes due to saturation lead to considerable changes in seismic properties such as velocity, density and bulk modulus of the reservoir. Gassmann's model (Gassmann 1951; Wang 2001; Smith et al., 2003; Kumar and Mohan 2004; Mavko et al., 2009; Avseth et al., 2010; Dimri et al., 2012) is being mostly used to predict P and S wave velocities with respect to changes in saturation. The changes in seismic properties of the reservoir are being manifested on time-lapse seismic data either in the form of time shifts or amplitude variations or both. Depending upon the reservoir condition, data quality and repeatability issues, time-lapse amplitude analysis may or may not compliment the time-lapse time shift analysis. In the case of Gulfaks oil field in North Sea, amplitude analysis is found to be more useful as compared to the time shift analysis (Landro et al., 1999). The aim of present study is to understand how would be the time-lapse seismic response of a paysand of the Ankleshwar reservoir in Cambay basin, India, which is a target for $CO_2$ – EOR. In pursuance of the same, synthetic seismic modeling based on well logs and Gassmann's fluid substitution analysis is carried out to study the effect of saturation changes in synthetic seismic data. It is observed that the top of the reservoir will experience a detectable time shift after injection of $CO_2$ into the reservoir and time-lapse time shift analysis would be more helpful compared to the amplitude analysis. The generation of synthetic sonic and density logs and synthetic seismic trace at variable saturations of $CO_2$ is carried out by using Hampson-Russel software. The overall drop in P-wave velocity and P-impedance is estimated by using MATLAB code for Gassmann's fluid replacement analysis.

## THE STUDY AREA

The study area, Ankleshwar oil field is one of the major oil producing fields of Cambay basin, India. In the field, Tertiary sediments varying in thickness between 1343 and 2026 m have been deposited over Deccan trap basement (Mukherjee, 1981).The Ankleshwar formation, which is deposited in marine regression phase during Middle to Upper Eocene age (Chowdhary 2004; Holloway et al., 2007), is a major reservoir unit in the field. The Ankleshwar reservoir consists of sandstone, shale and siltstone layers. The reservoir is subdivided into four major stratigraphic units viz., Telwa shale, Ardol, Kanwa shale and

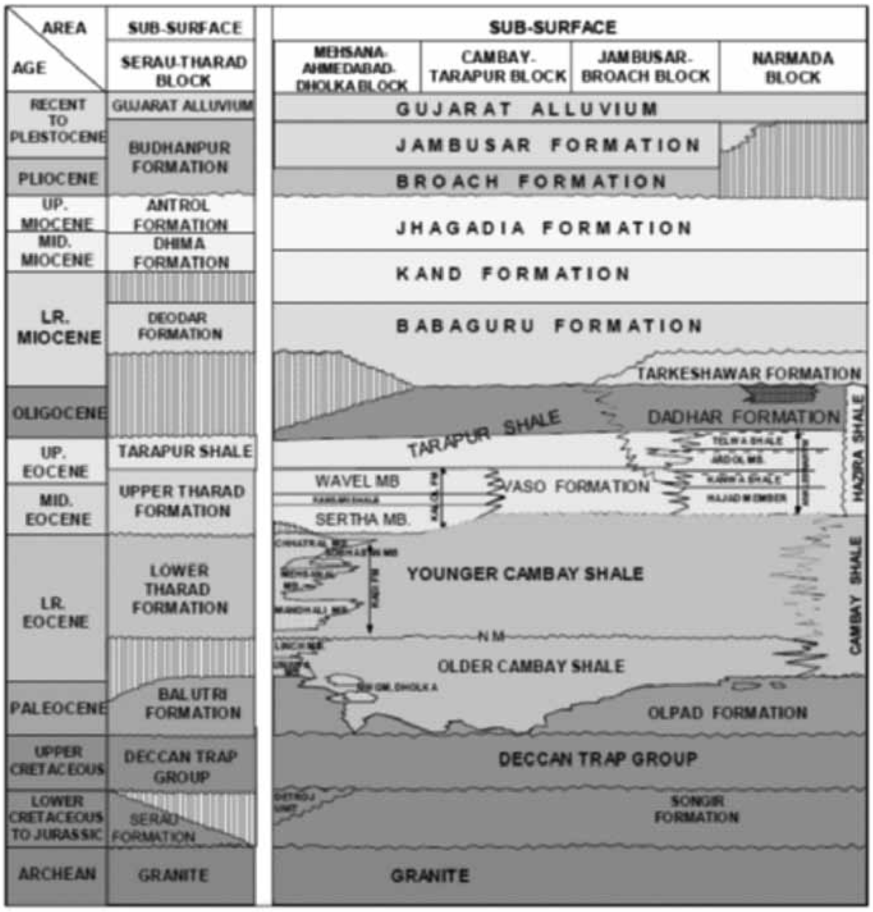


**Figure 1.** The generalized stratigraphy of the Cambay basin showing stratigraphy of the Ankleshwar formation (www.dghindia.org).

Hazad members (Figure 1). The Ardol and Hazad members are recognized as sandstone units, however, they contain shale laminae in between. Hazad member hosts the main recoverable reserves of oil. Hazad and Ardol members together are divided into eight sand layers, viz., $S_1$,$S_2$, $S_{3+4}$, $S_5$, $S_{6+7}$, $S_{8+9}$, $S_{10}$ and $S_{11}$ from bottom to top. Sand layer "$S_{3+4}$" is the major producer in the field.

The field has been producing oil and gas since 1961. In 1966, the secondary recovery process, water injection was started to restore the declined reservoir pressure. Now, the production has substantially declined and the water cut is more than 90%. The operator, Oil and Natural Gas Corporation (ONGC) Ltd., has a strategy for $CO_2$ – EOR to increase the life of field. A mixture of $CO_2$ and other hydrocarbon gasses (methane, ethane, propane and butane) will be injected into paysands $S_{3+4}$ and $S_5$ for EOR. The vertical succession of $S_{3+4}$, $S_5$ sands and Kanwa interval in a well $W_6$ is shown in Figure 2. The tops of these layers are taken from the formation evolution reports provided by the operator. The interpretation is mainly based on gamma ray log. The intervals with gamma ray counts less than 65 API and greater than 65 API represent sand layers and shale layers, respectively. As illustrated in Figure 2, the sand layer $S_5$ is subdivided into nine layers viz., $S_{5\text{-}1}$, shale2, $S_{5\text{-}2}$, shale3, $S_{5\text{-}3}$, shale4, $S_{5\text{-}4}$, shale5, $S_{5\text{-}5}$ from bottom to top due to the presence of interbedded shale layers.

Since reservoir modeling and simulation studies carried out by NGRI, India and SINTEFF, Norway (Srivastava et al., 2012, Dimri et al., 2012) with support from ONGC Ltd., India recommended the Ankleshwar reservoir for $CO_2$ – EOR, we tried to do a feasibility assessment of time-lapse seismic to monitor $CO_2$ that needs to be injected into the reservoir. We try to address the following questions based on Gassmann's fluid substitution analysis and seismic forward modelling using well logs:

1. Can the changes in Ankleshwar reservoir due to replacement of oil and water with $CO_2$ be manifested on time-lapse seismic data?
2. Will the changes in reservoir condition lead to either time-shift or amplitude variation in post injection seismic data?
3. Can the changes due to fluid replacement be detectable within the seismic resolution limit?
4. Will the time-lapse seismic monitoring of $CO_2$ movement in this reservoir be feasible?

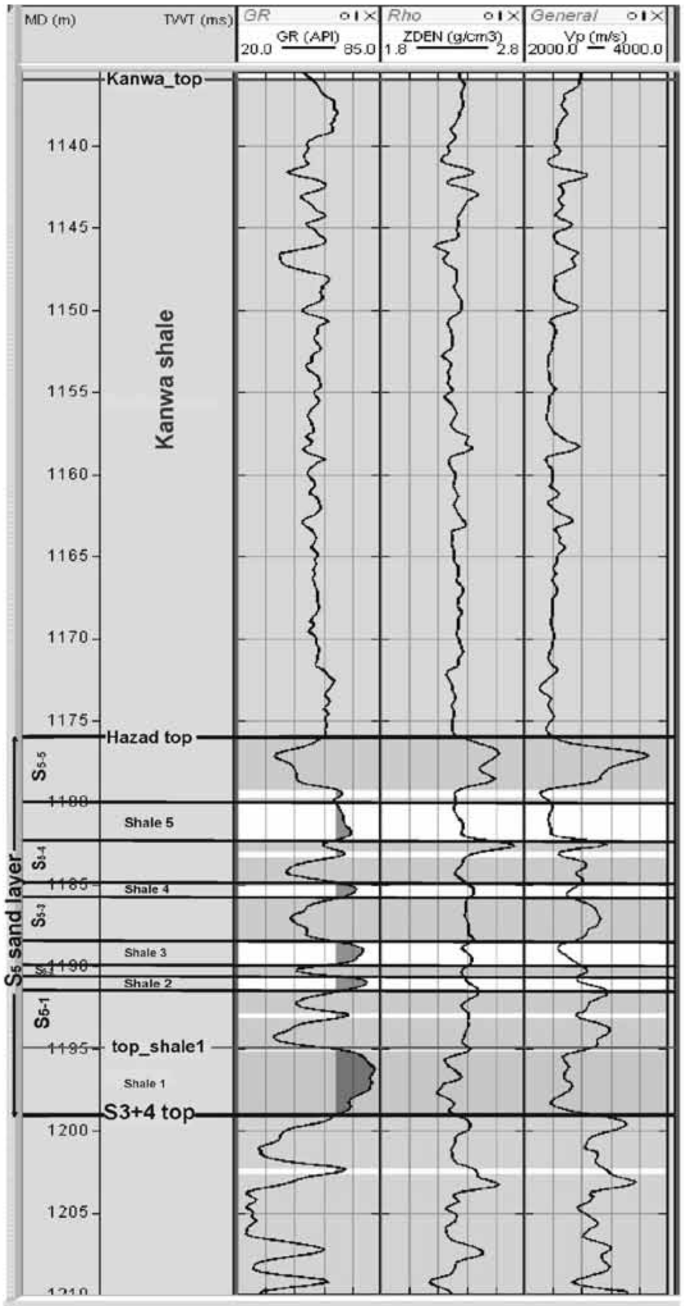


**Figure 2.** The vertical succession of Kanwa interval, $S_5$ sand, shale1 and $S_{3+4}$ sand layers identified on gamma ray, density and sonic logs of well $W_6$. Dark intervals represent shale laminae. The sublayers of the $S_5$ sand layer are also demarcated on the figure.

## Time-Lapse Seismic Response Evaluation for Ankleshwar Reservoir

To estimate the time-lapse seismic response of the reservoir after the replacement of oil and water in the reservoir with $CO_2$, a well $W_6$ drilled through $S_5$ paysand is chosen for analysis as required sonic log was available for this well. The reservoir properties required for Gassmann's fluid substitution analysis are taken from the production data and other information provided by the operator. According to reservoir simulation result, initial water saturation at the time of $CO_2$ injection is 60% (Ganguli et al., 2014). As the initial water saturation is 60% and since the reservoir has no gas cap (Srivastava et al., 2012) the remaining 40% of pore space can contain oil. The average porosity of $S_5$ sand layer is 24%, the irreducible water in the reservoir is 20% and residual oil saturation is 20% (information provided by the operator). Thus, for the most feasible case out of 40%, only 20% of remaining oil can be produced using $CO_2$ – EOR. Injection of $CO_2$ increases oil production

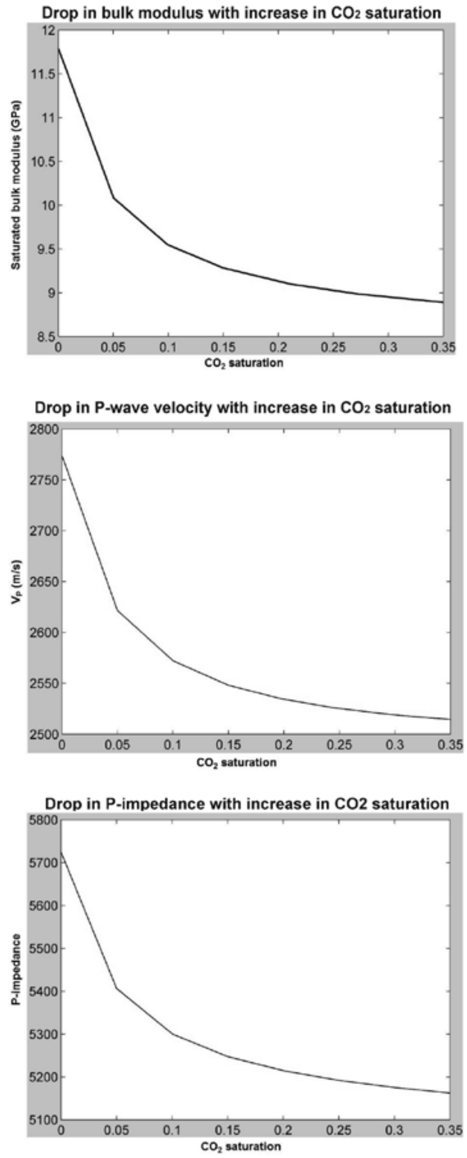


**Figure 3.** The figure illustrates the abrupt drop in saturated bulk modulus, P-wave velocity and P-impedance until $CO_2$ saturation is 15%.

and reduces water production. Out of the 40% producible water, on an average 15% will be produced (Ganguli et al., 2014) after $CO_2$ injection. Thus, $CO_2$ has to replace 20% oil and 15% water, hence the maximum $CO_2$ saturation in the sand layer can be 35%.

The physical properties of $CO_2$ with reservoir condition of $S_5$ sand layer at 75°C temperature and 121.6kg/cm$^3$ pressure are computed using Batzle and Wang (1992) equations. Since S-wave velocity information is not available, dry rock poisson's ratio 0.1 is used for computation of dry rock modulus or frame bulk modulus ($K_d$). For computation of the matrix bulk modulus ($K_m$), composition of $S_5$ sand layer (Figure 2) is considered as 90% quartz and 10% clay. The physical properties of $S_5$ sand layer used in fluid substitution modeling are given in Table 1.

Injected $CO_2$ accumulates under the cap of the reservoir and thickens downward by replacing insitu fluids. Thus, the effect of variation in thickness as well as saturation is studied. The liquids in $S_5$ sand layer are systematically replaced by $CO_2$ in steps of 5% increase in saturation. The thickness of $CO_2$ in the target zone has gradually increased downward from 0 m to 18 m in steps of 3 m. The target zone is 18 m thick (top at 1176m and bottom at 1194m) (Figure 2), which means $CO_2$ gas has occupied entire paysand. To carry out forward modeling, velocity and density structure of the reservoir at initial saturation conditions is available from the sonic and density logs. For each value of $CO_2$ saturation,

**Table 1.** The physical properties of $S_5$ sand layer used for analysis

| Parameter | Value |
|---|---|
| Reservoir temperature | 75ºC |
| Reservoir pressure | 121.6 $Kg/cm^2$ |
| Bubble Point Pressure | 90.5 $Kg/cm^2$ |
| Water saturation | 60% |
| Oil saturation | 40% |
| Bulk modulus of Oil | 1 GPa |
| Bulk modulus of water/brine | 2.38GPa |
| Bulk modulus of $CO_2$– gas | 0.06149Gpa |
| Density of oil | 750 $Kg/m^3$ |
| Density of water/brine | 1090 $Kg/m^3$ |
| Density of $CO_2$ - gas | 373 $Kg/m^3$ |

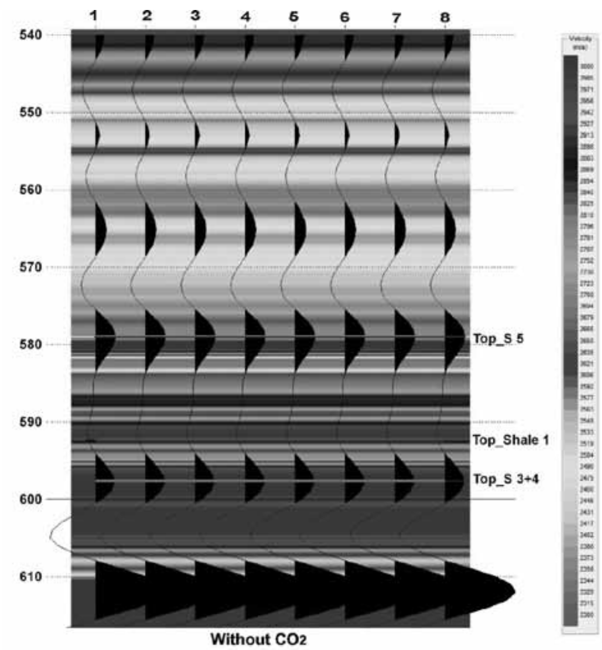


**Figure 4.** Baseline seismic data (a single trace is repeated many times in order to display it as data) generated from the initial values of saturation in the paysand. Gray scale represents P-wave velocity. Top of $S_5$, top of Shale 1 and top of $S_{3+4}$ are shown on synthetic data with horizontal lines.

synthetic sonic and density logs are generated. To monitor the seismic response of the paysand $S_5$ with changes in fluid saturation, a Ricker wavelet of 50 Hz frequency is convolved with reflectivity series and zero offset synthetic seismic traces are generated. The synthetic seismic traces generated without $CO_2$ in the paysand are considered as baseline data. Synthetic seismograms generated for varying saturation and for different thicknesses of $CO_2$ in the reservoir represent monitor data.

To estimate the average velocity drop in the $S_5$ sand layer, an average value of 2774 m/s obtained from sonic log is used as initial P-wave velocity for Gassmann fluid substitution analysis using MATLAB code. A Change in P-wave velocity, P-impedance and bulk modulus with the increase in $CO_2$ saturation is studied. The percentage drop in P-wave velocity and P-impedance of the paysand $S_5$, due to replacement of oil and water with $CO_2$ is estimated.

## RESULTS

Steep drop in saturated bulk modulus, P-wave velocity and P-impedance is observed until $CO_2$ saturation reaches 15%. After that stage variation in these quantities is subtle (Figure 3). As $CO_2$ saturation reaches 35%, P-wave velocity drops by 9% and P-impedance drops by 10%. Figure 4 illustrates the baseline seismic data, which represents the paysand without $CO_2$. Figure 5 illustrates the synthetic seismic data sets modeled at variable saturations of $CO_2$

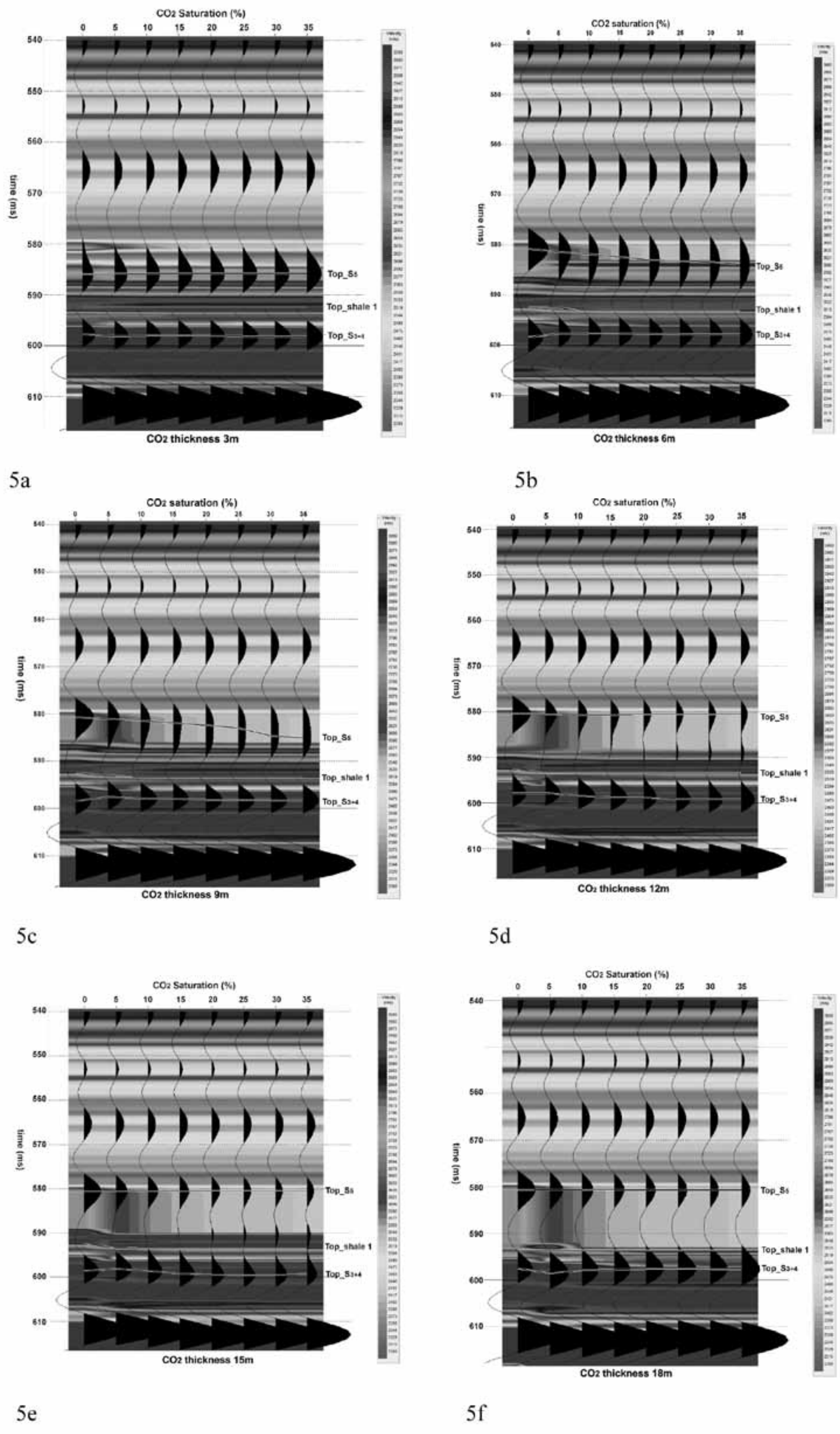


**Figure 5.** Modeled P-wave velocity with gray scale and synthetic seismic traces for varying saturation and thickness of $CO_2$; a-f represent monitor data with 3 m, 6 m, 9 m, 12 m, 15 m and 18 m thickness of $CO_2$, respectively. Figure 5a clearly shows 6 ms time shift of the top compared to the baseline case (Figure 4). Figure 5e shows 2 ms time shift at the top and bottom of $S_5$ layer and at the top of $S_{3+4}$. Figure 5f reveals that top of Shale 1 interferes with the top of $S_{3+4}$ as $CO_2$ occupies full thickness of the sand layer. Figures 5d and 5e show a sub horizontal reflector between top_$S_5$ and top_Shale 1.

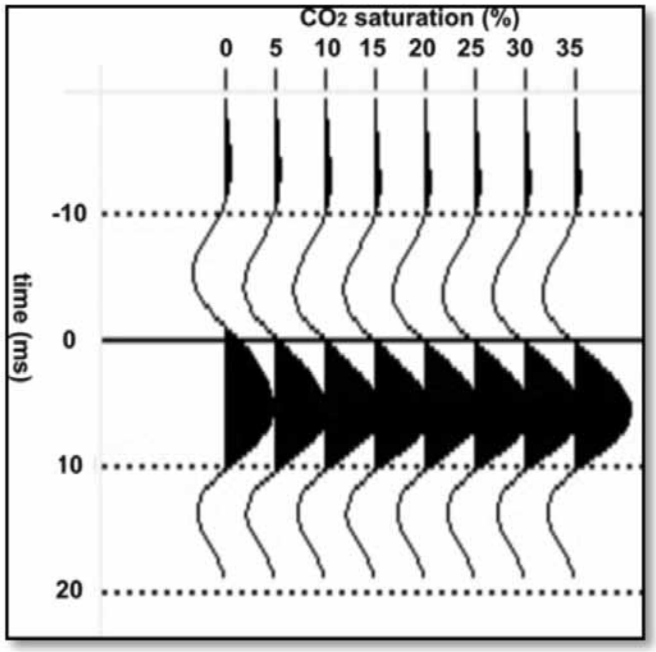


**Figure 6.** The cross-correlation output of base data with monitor data representing the paysand occupied by 3m thickness of $CO_2$. The cross-correlation peak is at 6 ms.

in the paysand. In Figures 4 and 5, background gray scale represents modeled P-wave velocity. As shown in Figure 5a to Figure 5e, in the time window 580 ms to 598 ms, darker region decreases with increase in saturation, which indicates a drop in velocity with $CO_2$ saturation in the target zone. This velocity drop leads to the reduction in acoustic impedance difference between Kanwa shale and $S_{5\text{-}5}$ sand layer and also between $S_{5\text{-}1}$ sand and shale 1 (Figure 2). At initial saturation conditions, i.e. without $CO_2$ in the paysand, the top reflector of the paysand (Top_$S_5$) is at 580 ms and the bottom reflector (top_shale1) is at 592 ms (Figure 4). After the first appearance of $CO_2$ in the paysand, i.e. when it occupies 3 m thickness of the paysand, the top reflector is pushed down by 6 ms and the bottom reflector (shown as top_shale1 on Figure 5a) is pushed down by 2 ms. However, as gas thickness increases in the paysand, time shift at the top reservoir reduces to 2 ms (Figures 5d-f). Careful observation of Figure 5d and Figure 5e shows another sub-horizontal reflector at the bottom of $CO_2$ plume, which is between top of $S_5$ and top of shale 1. As illustrated in Figure 5f, when $CO_2$ had occupied entire paysand, top_shale1 has interfered with top_$S_{3+4}$.

## DISCUSSION

Replacement of oil and water in the $S_5$ paysand of the Ankleshwar reservoir with $CO_2$ using Gassmann's equation and available information infers that there could be 9% drop in P-wave velocity for 35 % of $CO_2$ saturation. The injection of $CO_2$ into $S_5$ paysand can cause substantial changes in bulk modulus, the P-wave velocity and P-impedance until its saturation reaches 15%. The variation in these quantities becomes subtle beyond 15% saturation. The synthetic seismic modeling exercise carried out for the $S_5$ sand layer in a well ($W_6$) of Ankleshwar reservoir predicts that injection of $CO_2$ into the paysand will lead to push down effect at the top and the bottom of the reservoir. However, fluid replacement effect will be more visible at the top reflector and should give rise to observable time shift (6 ms) on the real time-lapse seismic data. Due to the first appearance of $CO_2$ in the topmost 3 m of the paysand there will be 6 ms push down effect at the top. In the present study, the push down effect at the top is due to the reduction in the acoustic impedance of the paysand with respect to overlying Kanwa shale formation. The actual top of the paysand at 580 ms on baseline data could be mapped at 586 ms on monitor data, because acoustic impedance difference is large enough to cause a reflection at 586 ms. The reflection event at 586 ms can be considered as apparent top of the paysand "$S_5$". However, as gas occupies full thickness of the paysand, the time shift at the top reduces to 2 ms (Figure 5 d-f). Hence, we can infer that the first monitor survey should be acquired before $CO_2$ occupies full thickness of the paysand. The maximum time shift at the bottom of the paysand $S_5$ is only of the order of one sample (2 ms) (Figure 5 c-f) and also the bottom reflector (Top-Shale 1) interferes with the top of the sand layer "$S_{3+4}$" (Figure 5f), when $CO_2$ occupies full thickness of the paysand. Thus, the time shift of the bottom of the paysand may not be resolved in real time-lapse seismic

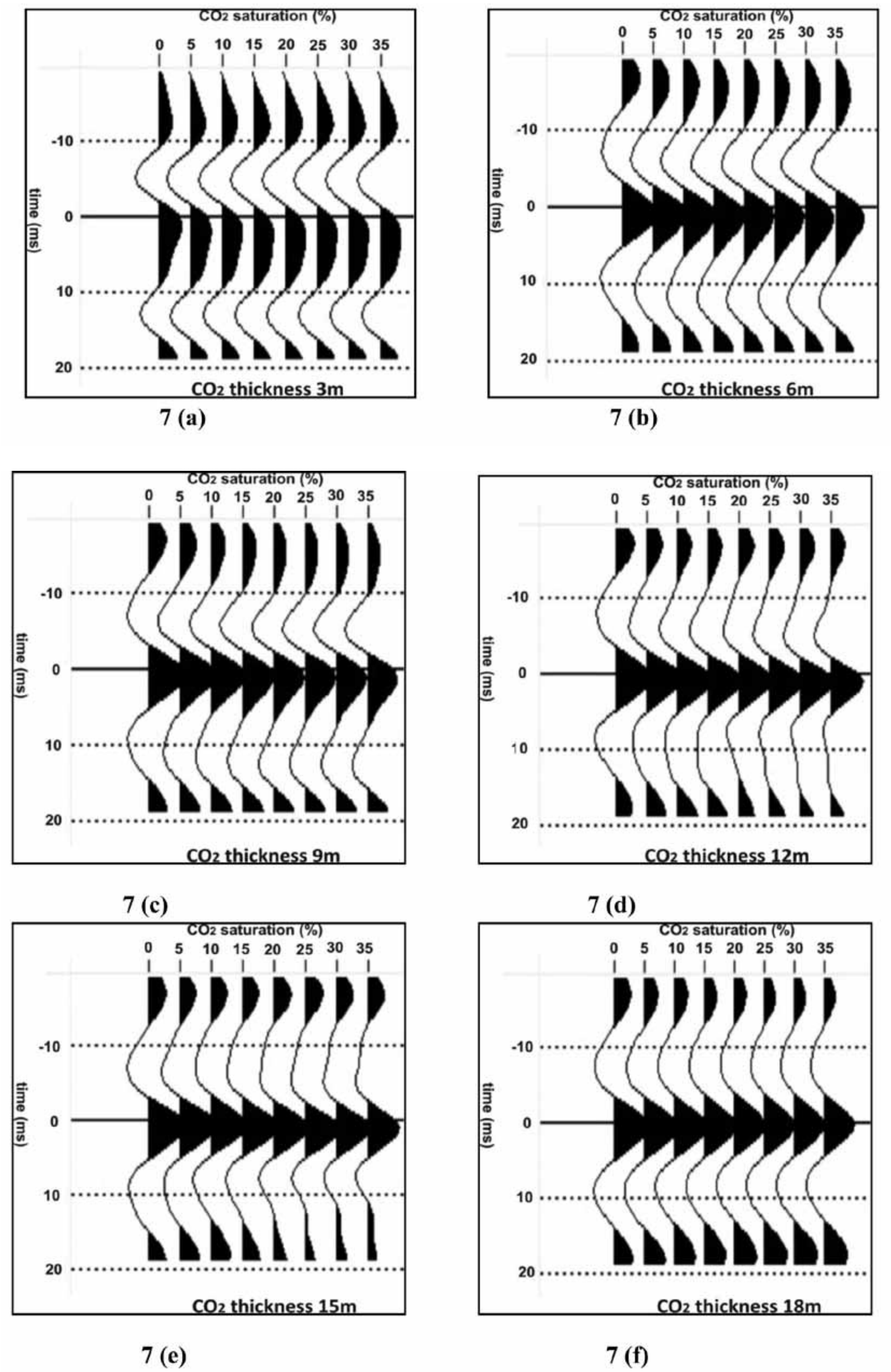


**Figure 7.** Cross-correlation output of base data with monitor data sets modeled at 3 m, 6 m, 9 m, 12 m, 15 m and 18 m thickness of $CO_2$ inside the $S_5$paysand. In Figure a cross-correlation peak is at 2 ms and in b-f cross-correlation peak has gradually moved towards 0 ms.

studies. The drop in acoustic impedance difference of the paysand with respect to Kanwa shale and shale1 layers due to injection of $CO_2$ will lead to a reduction in amplitude of top reflector. Thus, in this case time-lapse amplitude analysis may not be much helpful. Below the $CO_2$ plume a sub-horizontal reflection occurs due to acoustic impedance contrast between the $CO_2$ saturated paysand and the remaining paysand. This sub horizontal reflector would help to monitor $CO_2$ movement in the reservoir.

In the absence of data from major paysand $S_{3+4}$, this analysis was carried out for another paysand $S_5$. If the operator injects $CO_2$ into the sand layer "$S_{3+4}$", similar results will be generated because similar to the sand layer "$S_5$", the $S_{3+4}$ sand layer is also overlaid by a lower velocity shale layer (Shale 1). Thus, in this case also injection of $CO_2$ will lead to reduction in acoustic impedance difference between $S_{3+4}$ sand layer and shale 1 layer and amplitude analysis may not be helpful in detecting time-lapse changes. The maximum time shift 6 ms at the top of $S_5$ paysand is due to the first appearance of $CO_2$ in high velocity, $S_{5\text{-}5}$ sub layer (Figure 2), which is underlain by low velocity shale 5 sublayer. Such kind of velocity sub layering inside $S_5$ sand layer made fluid substitution effect more prominent at the top. In case of sand layer "$S_{3+4}$" there is no such velocity sub layering, thus, the magnitude of time shift at the top might be lower than that of $S_5$ sand layer. The sub layers inside $S_5$ sand layer could not be detected on synthetic seismic section. The velocity sub layering detected on sonic log could add additional information for the interpretation.

In the present study, synthetic modeling is carried out at a single well because of the limited information available. We are aware that for a comprehensive evaluation, Synthetic modeling should be done for the entire reservoir for estimation of time shifts. We also believe that real data will be different from the synthetic one because of noise and other assumptions. The noise in real data may obscure the sub-horizontal reflector below the $CO_2$ plume and it might go undetected. We have seen that maximum changes are observed at 15% gas saturation, but it would be interesting to estimate the time $CO_2$ plume will take to attain 15% saturation.

The quality check of the results is performed. Base data is cross correlated with the monitor data sets to verify time shift at the top and bottom of the paysand $S_5$. Cross-correlation of baseline data with monitor data modeled for the paysand occupied by 3 m thick $CO_2$ is done in time window of 570 ms to 590 ms, which covers the top reflector of the paysand. In Figure 6 the cross-correlation peak is at 6 ms, which infers that due to the first appearance of $CO_2$, the top of the paysand is pushed down by 6 ms. In order to quantify the time shift at the bottom of the $S_5$ paysand, cross-correlation of base and monitor data sets is done in the time window covering whole paysand, time window 570 ms to 600 ms. Figures 7a-f represent the cross-correlation outputs for 3 m, 6 m, 9 m, 12 m, 15 m and 18 m thick $CO_2$ plume in the $S_5$ paysand. In Figure 7a the central cross-correlation peak is at 2 ms, which represents that bottom of the paysand was pushed down by 2 ms, when $CO_2$ had occupied 3 m thickness of the paysand. As illustrated in Figure 7b-f with increase in thickness of $CO_2$ in the paysand, the central cross-correlation peak has gradually moved towards zero. In Figures 7a-f time shift is maximum at maximum $CO_2$ saturation.

The observed time shift at the bottom of the paysand is verified from the observed velocity drop (9% of the initial velocity) using the empirical relation developed by Landrø and Stammeijer (2004). The relation between relative time shift and relative velocity drop is given as:

$$\frac{\Delta T}{T} = \frac{-\Delta V}{V} \qquad \text{................ (1)}$$

Where, V is the initial average velocity of the reservoir, ΔV is the velocity drop and T is the two way time thickness of the paysand, which is given as below

$$T = \frac{2Z}{V} \qquad \text{................ (2)}$$

Where, Z is the thickness of the zone. After the substitution of initial velocity and estimated velocity drop into the above equations the theoretical time shift is found to be 2 ms. The theoretically predicted time shift (ΔT) at the bottom of the paysand, 2 ms matches with the observed value on synthetic seismic data.

## CONCLUSIONS

Injection of $CO_2$ under miscible conditions into the $S_5$ sand layer of the Ankleshwar reservoir will lead to detectable time shift at the top. The time-lapse time shift analysis would be more helpful as compared to the time-lapse amplitude analysis for detection of time-lapse changes, as fluid substitution leads to reduction in acoustic impedance difference. The monitor seismic survey would image $CO_2$ plume as a sub-horizontal reflector below $CO_2$ saturated sand. Hence, time-lapse seismic monitoring of injected $CO_2$ in the Ankleshwar reservoir is feasible.

## ACKNOWLEDGEMENT

The authors are thankful to the Director, CSIR-NGRI for permission to publish this work. They are indebted to Norwegian embassy, New Delhi for financial support through Indo-Norwegian research project. They thank ONGC Ltd., India for providing data to carry out this work. Useful suggestions by reviewers and Chief Editor are gratefully acknowledged.

## Compliance with Ethical Standards

The authors declare that they have no conflict of interest and adhere to copyright norms.

## REFERENCES

Avseth, P., Mukerji, T., and Mavko, G., 2010. Quantitative seismic interpretation: Applying rock physics tools to reduce interpretation risk. Cambridge University Press.

Chowdhary, L. R., 2004. Petroleum Geology of the Cambay Basin, Gujarat., India. Indian Petroleum Publishers.

Dimri, V., Srivastava, R. P., and Vedanti, N., 2012. Fractal models in exploration geophysics: applications to hydrocarbon reservoirs, Elsevier., v.41.

Ganguli, S. S., Vedanti, N., Akervoll, I., and Bergmo, P., 2014, January. An estimation of $CO_2$-EOR Potential from a sector model in a mature oil field, cambay Basin, India. In Annual convention, IGU-Kurukshethra, 2014.

Gassmann, F., 1951. Über die elastizität poröser medien: Vierteljahrss-chrift der Naturforschenden Gesellschaft in Zurich. Paper translation at http://sepwww. Stanford. edu/sep/berryman/PS/gassmann. pdf., v.96, pp: 1-23.

Holloway, S., Garg, A., Kapshe, M., Pracha, A.S., Khan, S.R., Mahmood, M.A., Singh, T. N., Kirk K.L., Applequist, L.R., Deshpande, A., Evans, D.J., Garg, Y., Vincent, C.J., and Williams, J.D.O., 2007. A regional assessment of the potential for CO2 storage in the Indian subcontinent, Sustainable and Renewable Energy Programme Commissioned Report CR/07/198 by British Geological Survey (BGS). Sustainable and Renewable Energy Programme Commissioned Report CR/07/198, British Geological Survey (BGS), NERC.

Kumar, A., and Mohan, S., 2004. Feasibility Assessment of a Time-Lapse Seismic Survey for Thermal EOR in Balol Field, India, Based on Rock Physics and Seismic Forward Modeling. In Proceedings of the 5th International Conference and Exposition on Petroleum Geophysics, Society of Petroleum Geophysicists, pp: 688-695.

Landrø, M., Solheim, O. A., Hilde, E., Ekren, B. O., and Strønen, L. K., 1999. The Gullfaks 4D seismic study. Petroleum Geoscience, v.5, no.3, pp: 213-226.

Landrø, M., 2002. Uncertainties in quantitative time-lapse seismic analysis.Geophysical Prospecting, v.50, no.5, pp: 527-538.

Mavko, G., Mukerji, T., and Dvorkin, J., 2009. The rock physics handbook: Tools for seismic analysis of porous media. Cambridge university press.

Mukherjee, M. K., 1981. Evolution of Ankleshwar anticline, Cambay Basin, India.

Smith, T. M., Sondergeld, C. H., and Rai, C. S., 2003. Gassmann fluid substitutions: A tutorial. Geophysics, v.68, no.2, pp: 430-440.

Srivastava, R. P., Vedanti, N., Dimri, V. P., Akervol, I., Bergmo, P., and Biram, R. S., 2012, November. CO 2-EOR: A Feasibility Study of an Indian Oil Field. In 2012 SEG Annual Meeting. Society of Exploration Geophysicists.

Wang, Z., 2001. Fundamentals of seismic rock physics. Geophysics, v.66, no.2, pp: 398-412.